Moroccan Journal of Chemistry
ISSN: 2351-812X
http://revues.imist.ma/?journal=morjchem&page=login
M. Bencheikh / Mor. J. Chem. 4N°4 (2016) 996-1003

Study of 6 MV Photon Beam Dose Profiles and Investigation of Jaw Motion Effects on the Beam Dose Profiles and the Dose Delivered in a Water Phantom

Mohamed BENCHEIKH[1], Abdelmajid MAGHNOUJ[1], Jaouad TAJMOUATI[1] and Yassine BENKHOUYA[2;3]

1 : LISTA Laboratory, Physics Department, Faculty of Sciences Dhar El-Mahraz, University of Sidi Mohamed Ben Abdellah, Fez, Morocco.

2: Nuclear physics laboratory, Faculty of sciences Agdal, university of Mohammed V, Rabat, Morocco"

3 : Radiotherpay department, clinic al kawtar, Fez, Morocco"

Abstract

This study investigated the medical linear accelerator jaw motion effects on the delivered dose. The focus was to examinate the photon beam dose profiles as a function of the jaw motion and depending on the depth in the water phantom along the central beam axis and the irradiation field sizes. The measurements of dose profiles were performed for a 6 MV photon beam in a water phantom, the field sizes of 3×3 cm², 4×4 cm², 6×6 cm², 8×8 cm², 10×10 cm², 12×12 cm², 15×15 cm², 20×20 cm², 25×25 cm², 30×30 cm², and 35×35 cm² at depth of 1.5 cm, 5 cm, 10 cm, 20 cm, and 30 cm on the central beam axis, and source-to-surface distance (SSD) of 100 cm for Varian Clinac 2100 linear accelerator. The purpose of this study was to investigate the jaw motion effects on the dose profiles and subsequently on the delivered dose depending on the field size and depth in the water phantom and also the beam dose profiles' symmetry about the central beam axis. We proceeded to calculate two parameters: the normalized width and the difference of the width between the left and right width of dose profiles as a function of the field size and depth along the central beam axis. We have shown that the motion of the jaws to define the irradiation field size have impacts on the beam dose profiles and its symmetry. the spread of the width difference was in a wave motion along the central beam axis and within a range of off-axis distance from -2 mm to 2 mm, which it should be considered in the treatment of tumors and spare the healthy cells.

** Corresponding author: bc.mohamed@gmail.com*

Received 05 Sept 2016, Revised 26 Dec 2016, Accepted 02 Jan 2017

***Keywords**: Jaw motions, Dose Profile, Photon Dosimetry, Contamination Electrons.*

Introduction:

Radiotherapy treatment basic purpose is the irradiation of a target volume of cancerous cells while minimizing the amount of radiation absorbed in healthy cells. The beam shaping is an important element to reduce the absorbed dose in healthy tissues and critical structures as the eyes, the testicles ...etc. Medical linear accelerators are generally designed to provide wide beam homogeneous photons which can be collimated to a variety of irradiation field sizes and shapes. The collimation system includes the primary collimator and the secondary collimator [1,4,7,8]. The secondary collimators or conventional collimators, they are also called the jaws, they are used to shape a rectangular treatment field, in our study, the fields were square, symmetrical, and centered about the central beam axis, the field sizes were 3×3 cm², 4×4 cm², 6×6 cm², 8×8 cm², 10×10 cm², 12×12 cm², 15×15 cm², 20×20 cm², 25×25 cm², 30×30 cm², and 35×35 cm². The photon beam is output and passed through a primary collimator and a flattening filter; the purpose of this filter is to provide a uniform beam. A set of jaws move and restrict the beam to the desired size. The photon beam collimators behave as a source of secondary electrons produced by the photon interaction with the inner surface material of the jaws; these electrons contaminate the photon beam and increase the skin dose [6,9-11]; and subsequently affect the dose profiles and the delivered dose. The beam dose profile is a fundamental parameter necessary for characterizing a radiation beam in the radiotherapy and the dose delivered to the patient. It is as a function of off-axis distance, and irradiation field size. The profiles at different depths are needed for the study of dosimetry; they are better obtained by using a water phantom [1-3,5]. In this work, the focus was on studying the dosimetric effects of the jaw motions on the dose profiles and its symmetry about the central beam axis for the field sizes of 3×3 cm², 4×4 cm², 6×6 cm², 8×8 cm², 10×10 cm², 12×12 cm², 15×15 cm², 20×20 cm², 25×25 cm², 30×30 cm², and 35×35 cm². at depth of 1.5 cm, 5 cm, 10 cm, 20 cm, and 30 cm on the central beam axis in the water phantom. The study was based on the beam dose profiles' examination as a function of depth along central beam axis, and as a function of field size. It was also to investigate the jaw motion effects on the beam dose profiles and subsequently on the delivered dose depending on the irradiation field sizes and the depth in the water phantom. We have proceeded to calculate two parameters: the normalized width and the width difference between the left and right width of dose profiles as a function of the field size and depth on the central beam axis.

Materials and methods:

The majority of medical linear accelerators has two photon beam collimators; a fixed primary collimator with a conical opening, defines the maximum angular spread of the photon beam and a secondary collimator is adjus**Table** to provide the desired irradiation fields. In this study we worked on the jaw motion when defining the irradiation field size for Varian Clinac 2100 linear accelerator. The study based on the examination of the width of beam profiles at left and right of the beam central axis and we investigated this parameter to check out the effects of the jaw motions on the photon beam dosimetry. In normal use, each pair of jaws is coupled to provide symmetric rectangular fields centered about the central beam axis. In our study, we worked on open, square, symmetrical, and centered fields about the central beam axis. The photon beam must be constrained to ensure that only the required part of the patient was irradiated. To meet the requirements of very low dose rates at a great distance beyond the radiation field edge, the accelerators have a primary circular collimator near the source and limit the field to a circular shape. The irradiation field sizes were defined by the jaws and they provide the irradiation field sizes from 3×3 cm² to 35×35 cm² in this work. The adjus**Table** collimators consist of two pairs of jaws, jaws X and jaws Y, one above the other and at right angles (**Figure** 1). The jaws were defining the size of the treatment field. They were usually made of flat-faced blocks of lead or tungsten that move in an arc in order that the face of the block shall be aligned with the field's divergent edge [1,4,8]. Inevitably, one of the collimator jaws will be closer to the source than the other (**Figure** 1). In this study,

the focus was on the examination of 6 MV photon beam dose profiles as a function of field sizes and depth in the water phantom along central beam axis. the measured dose profiles' data for field sizes of 3×3 cm², 4×4 cm², 6×6 cm², 8×8 cm², 10×10 cm², 12×12 cm², 15×15 cm², 20×20 cm², 25×25 cm², 30×30 cm², and 35×35 cm² at depth of 1.5 cm, 5 cm, 10 cm, 20 cm and 30 cm in the water phantom on the central beam axis. The SSD was of 100 cm, and photon beam energy was of 6 MV. The photons were interacted with the elements of the medical linear accelerator head components, and especially the beam modifiers as the primary and secondary collimators, and the flattening filter. The interactions produced the contamination electrons of the photon beam [6, 9-11]. These electrons deposited their energy in the water phantom and it contributed to the delivered dose, therefore they have effects on the beam dose profiles and percentage depth dose (PDD). In this work, we have calculated both widths at left profile and right profile, and then we calculated the normalized width in the first step, and the difference width in the second step. Finally we have plotted the variation of these parameters as a function of depth along the central beam axis and irradiation field sizes; the aim of this examination was to investigate the contamination electrons due to the jaw motions on the beam profiles and also on the beam symmetry along the central beam axis and subsequently the jaw motion effects on the beam dose profiles. We have worked on open (not wedged), square, symmetrical, and centered irradiation fields about the central beam axis

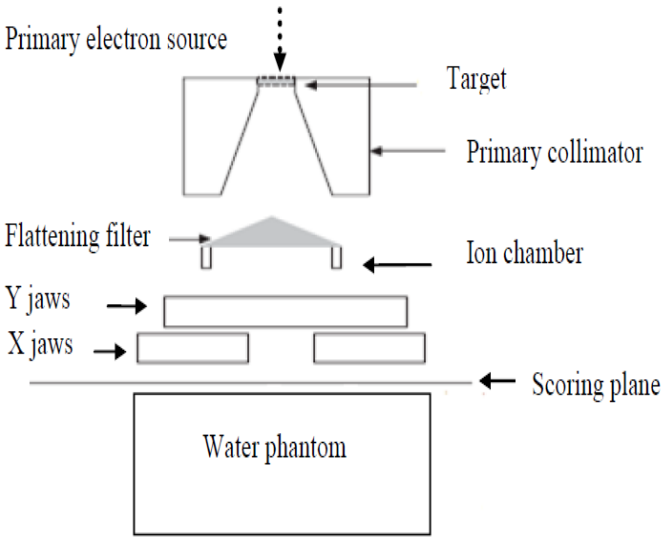

***Figure** 1: Medical linear accelerator head component geometry.*

Results and discussion:

To analyze the beam dose profiles, they were normalized for all irradiation field sizes and depths to 100% on the central beam axis. **Figure** 2 shows the dose profiles of the 6 MV photon beam for a field size of 10×10 cm² at different depths on the central beam axis. It can be seen in **Figure** 2 that the dose profiles were depended on the depth on the central beam axis; the curves of the dose profiles were widened more to more as the depth increased due to an inverse square law (ISL) that it was the relationship between the depth and the beam divergence. Next, the dose profiles were graphed for the irradiation field sizes of 3×3 cm², 4×4 cm², 6×6 cm², 8×8 cm², 10×10 cm², 12×12 cm², 15×15 cm², 20×20 cm², 25×25 cm², 30×30 cm², and 35×35cm² in same **Figure** (**Figure** 3) It can be seen from **Figure** 3 that the dose profiles were depended on the irradiation field sizes; the dose profiles for larger field size were wider than the small field size.

To demonstrate the jaw motion effects on the dose profiles, we proceeded to calculate the left profile widths and right profile widths to a dose of 80% of the maximum dose. We introduced a normalization of the width (W_n) that was the quotient of the difference between left profile widths and right profile widths to the sum of these widths in absolute value that was shown by the following formula:

$$W_n = \left| \frac{W_l - W_r}{W_l + W_r} \right| \qquad (1)$$

where,

W_l: The left width corresponds to the left off-axis distance to 80% of the maximum dose on the central beam axis.

W_r : The right width corresponds to the right off-axis distance to 80% of the maximum dose on the central beam axis.

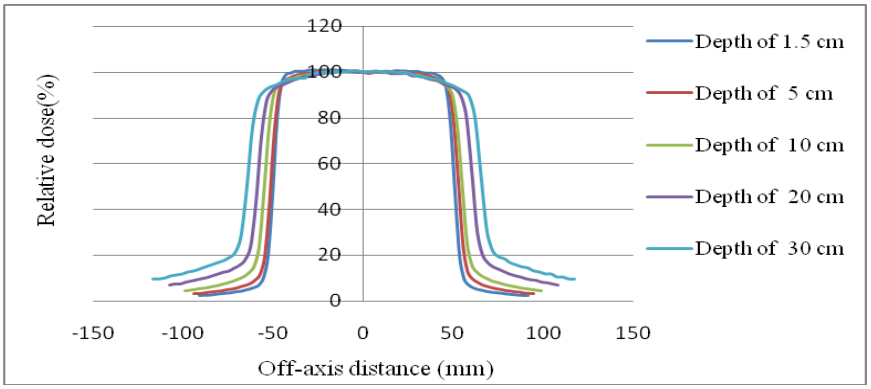

***Figure** 2: Dose profiles of 6 MV photon beam produced by Varian Clinac 2100 linear accelerator as a function of off-axis distance in the water phantom for field size Ad of 10×10 cm²; depths of 1.5 cm, 5 cm, 10 cm, 20 cm, and 30 cm; and SSD of 100 cm.*

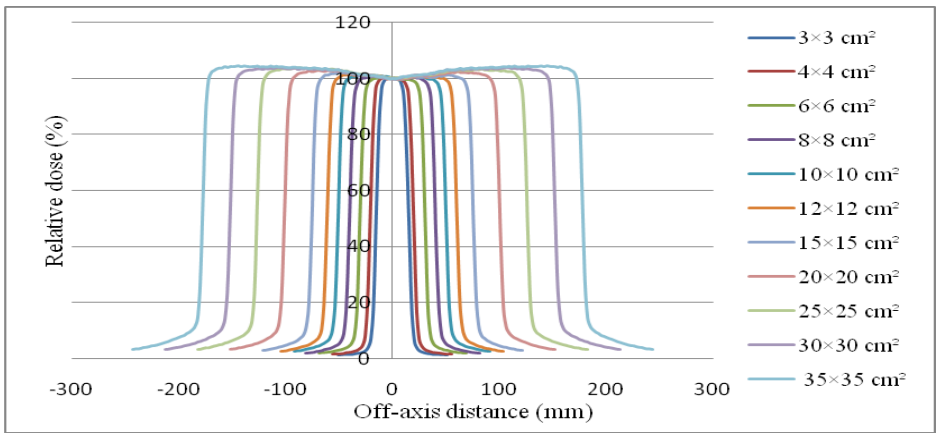

***Figure** 3: Dose profiles of 6 MV photon beam produced by Varian Clinac 2100 linear accelerator as a function of off-axis distance in the water phantom for field size Ad of 3×3 cm², 4×4 cm², 6×6 cm², 8×8 cm², 10×10 cm², 12×12 cm², 15×15 cm², 20×20 cm², 25×25 cm², 30×30 cm², and 35×35 cm²; depth of 1.5 cm; and SSD of 100 cm.*

Table 1 show the normalized width W_n, left profile width W_l, and right profile width W_r as a functions of the field size at a depth of de 1.5 cm in the water phantom.

Field size	**Side of square field (cm)**	Left width W_l (mm)	Right width W_r (mm)	Normalized width W_n
3×3 cm²	**3**	12,96	12,24	$2{,}88\ 10^{-02}$
4×4 cm²	**4**	18,01	17,51	$1{,}43\ 10^{-02}$
6×6 cm²	**6**	35,47	27,85	$1{,}20\ 10^{-01}$
8×8 cm²	**8**	37,71	37,33	$5{,}02\ 10^{-03}$
10×10 cm²	**10**	48,15	47,86	$3{,}08\ 10^{-03}$
12×12 cm²	**12**	58,23	58,20	$3{,}15\ 10^{-04}$
15×15 cm²	**15**	73,49	73,24	$1{,}74\ 10^{-03}$
20×20 cm²	**20**	99,19	98,10	$5{,}53\ 10^{-03}$
25×25 cm²	**25**	124,85	123,80	$4{,}24\ 10^{-03}$
30×30 cm²	**30**	150,08	149,02	$3{,}54\ 10^{-03}$
35×35 cm²	**35**	175,81	174,90	$2{,}59\ 10^{-03}$

***Table** 1: Left profile width W_l, right profile width W_r and normalized width W_n for field size Ad of 3×3 cm², 4×4 cm², 6×6 cm², 8×8 cm², 10×10 cm², 12×12 cm², 15×15 cm², 20×20 cm², 25×25 cm², 30×30 cm², and 35×35 cm²; depth of 1.5 cm on the central beam axis.*

To investigate the dose distribution profiles, we put on the same graph the variation of the normalized width as a function of the side of square field size A_d for the depth of 1.5 cm, 5 cm, 10 cm, 20 cm and 30 cm in the water phantom on the central beam axis (**Figure** 4).

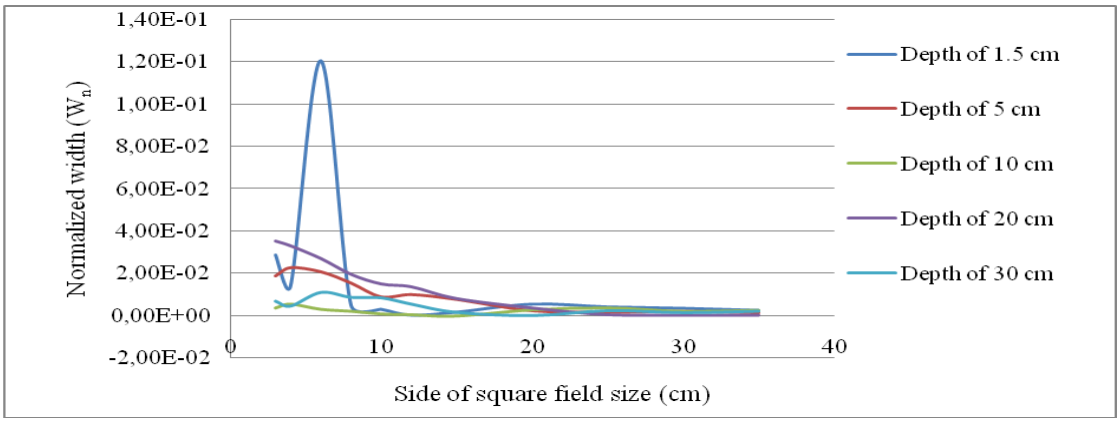

***Figure** 4: Variation of the normalized width W_n as a function of side of square field size for the depth of 1.5 cm, 5 cm, 10 cm, 20 cm and 30 cm in the water phantom on the central beam axis.*

The normalized width was greater for small field sizes than the larger field size; the normalized width curves for small field sizes were spaced between them as a function of depth. However, for the radiation field size great than the 20×20 cm²; the normalized width was very small and the normalized width curves were near to zero and close one to other for all studied depths (**Figure** 4). In small field sizes, the jaws were close together, the primary photons were interacted with the material constituting the jaw inner surface and the contamination electron were ejected by

Compton Effect [6]. The electron contamination passed through the phantom surface; the later was small for small field sizes, therefore, the electron contamination density was high and its dosimetry contribution to the total dose delivered was high also, therefore, the jaw motion for the small field size have an impact on the beam dose profile curves for small field sizes. A pair of collimator jaws will be closer to the source than the other making the electron distribution different at the beam edge. The contamination electrons deposited their energy in the traversed medium (water phantom); their paths in the medium are different which explains the space between the normalized width curves for each studied depth for small field sizes (**Figure** 4). In the large field sizes, the jaws were away from each other, the phantom surface crossing was large, so the density of contamination electron was low, hence, their dosimetric contribution to the dose delivered to the phantom was also low. So the normalized width curves were close one to other along the central beam axis (**Figure** 4). The difference between the left profile width and the right profile width was determined; this quantity allowed us to investigate the dose profile symmetry about the central beam axis as a function of depth in the water phantom.

Table 2 shows the difference between left profile width and right profile width as a function of depth and field size.

Depth	**Field size (cm²)**										
(cm)	**3×3**	**4×4**	**6×6**	**8×8**	**10×10**	**12×12**	**15×15**	**20×20**	**25×25**	**30×30**	**35×35**
1.5	0,725	0,507	7,620	0,376	0,296	0,037	0,256	1,092	1,053	1,060	0,910
5	-0,495	-0,823	-1,182	-1,197	-0,884	-1,203	-1,182	-0,516	-0,465	-0,695	-0,574
10	0,105	0,214	0,187	0,181	0,103	0,077	-0,001	0,608	0,998	0,702	0,992
20	-1,076	-1,397	-1,780	-1,745	-1,705	-1,871	-1,399	-0,848	-0,148	-0,112	-0,102
30	-0,229	-0,210	-0,786	-0,842	-1,035	-0,800	-0,282	0,000	0,721	0,508	0,887

***Table** 2: Difference between left profile width W_l and right profile width W_r as a function of depth for field size Ad of 3×3 cm², 4×4 cm², 6×6 cm², 8×8 cm², 10×10 cm², 12×12 cm², 15×15 cm², 20×20 cm², 25×25 cm², 30×30 cm², and 35×35 cm².*

To demonstrate the width difference variation, the **Figure** 5 illustrates a graphical presentation of the width difference variation as a function of depth in the water phantom for each field size.

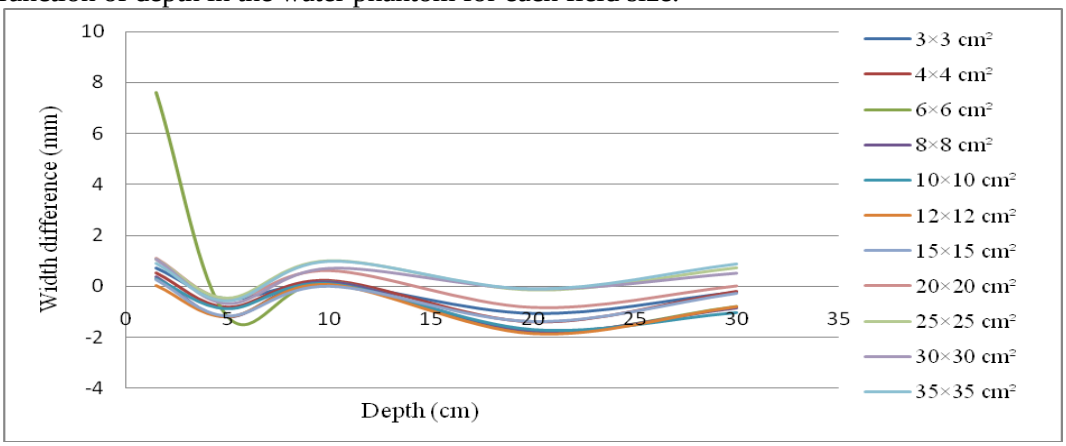

***Figure** 5: Variation of the difference between left profile width W_l and right profile width W_r as a function of depth for field size Ad of 3×3 cm², 4×4 cm², 6×6 cm², 8×8 cm², 10×10 cm², 12×12 cm², 15×15 cm², 20×20 cm², 25×25 cm², 30×30 cm², and 35×35 cm².*

The difference between the left profile width and right profile width was spread along the central beam axis as a wave motion about the central axis for all studied field sizes (**Figure** 5). In the shallow depths, the width difference curves were closer one to other, but when the depth increased in the water phantom, one was moved away from other. The difference variation of the width remains between -2 mm and 2 mm along the central beam axis (**Figure** 5).

Dose profiles are not symmetrical about the central axis even the irradiation field sizes were symmetrical. The beam dose profiles were symmetrical at same positions along the central beam axis in the water phantom for each studied field size. These points were defined by the intersection of the difference variation curves and the coordinate axis where the difference was zero and the dose profiles were not symmetrical elsewhere. The symmetry of dose profiles was depended on the irradiation field size and the depth along the central beam axis in the water phantom (**Figure** 5).

Conclusion:

The beam dose profile distributions were dependent on the jaw motions and the design of their inner surface that was responsible for the production of electron contamination. Recent linear accelerators are equipped with jaw where its inner surface designed of high atomic number materials, such as lead, tungsten.

In our work, we have shown that the jaw motion effects were very depending on the irradiation field size. Dosimetric contribution of electron contamination to delivered dose due to the jaw motion was more important in the small field sizes and it was almost zero in the field sizes great than 20×20 cm^2.

We have also shown that the dose profiles were not symmetrical about the central beam axis even the irradiation fields were symmetrical and centered about the central beam axis. The dose beam profiles symmetry varied with increasing depth on the beam central axis, for certain depths in the water phantom the difference width was zero and the beam dose profiles were symmetric. The interval variation of the difference with of the dose profile was from -2 mm to 2 mm along the beam central axis, thus, this interval was for the beam dose profile symmetry. Finally it can be concluded that the dose and the delivered dose profiles were affected by the design of the collimating system and the jaw motions. The later should be taken in consideration in the tumor volume treatment determination by the physician according to the IAEA protocols [12].

Acknowledgement:

The authors would like to thank Varian Medical Systems to allow us to use the dose profiles commissioning data of Varian Clinac 2100, and give us this opportunity to study the Varian linear accelerator technology and to participate in its future development, our study is one among many study over the world in this field.

References:

[1]: Mayles P., Nahum A., and Rosenwald J. C., 2007, Handbook of Radiotherapy Physics Theory and Practice, Taylor & Francis group, LCC, Unite State of America, pp 198 – 239 and pp 452 – 480.

[2]: Chang D. S., Lasley F. D., DAS I. J., Mendonca M. S., and Dynlacht J. R., 2014, Basic Radiotherapy Physics and Biology, Springer, New York, pp 77 – 92.

[3]: Podgorsak E.B., 2005, Radiation Oncology Physics: A Handbook For Teachers And Students, IAEA , Vienna, pp 161 – 216.

[4]: Karzmark C.J., Nunan C.S., and Tanabe E., 1993, Medical Electron Accelerators, Library of Congress, United States of America., pp 137 – 156.

[5]: Henriquez F. C. and Vargas-Castrillón S. T., 2007, A study on beam homogeneity for a Siemens Primus linac, Australasian Physical & Engineering Sciences in Medicine, Volume 30, Number 2, pp 147-151

[6]: Allahverdi M., Zabihzadeh M., Ay M.R., Mahdavi S.R., Shahriari M., Mesbahi A., Alijanzadeh H. , 2011, Monte Carlo estimation of electron contamination in a 18 MV clinical photon beam, Iran. J. Radiat. Res., Vol. 9 No. 1, pp 15 – 28.

[7]: Rafaravavy R., Raoelina A. and Bridier A., Study of dose distribution in high energy photon beam used in radiotherapy, HEP MAD' 07 International Conference, Antananarivo, Madagascar, 10 - 15 September 2007.

[8]: Bryan B. and George X X.,(2009), Monte Carlo modeling of a 6 and 18 MV Varian Clinac medical accelerator for in-field and out-of-field dose calculations: development and validation, Phys Med Biol. 2009 February 21; 54(4): N43–N57.

[9] Lonski P., Taylor M. L., Franich R. D. and Kron T., (2014), A collimated detection system for assessing leakage dose from medical linear accelerators at the patient plane, Australas Phys Eng Sci Med 37, pp 15–23.

[10]: Yang J., Li J. S., Qin L., Xiong W. and Ma C. M., (2004), Modelling of electron contamination in clinical photon beams for Monte Carlo dose calculation, Phys. Med. Biol. 49 , pp 2657–2673.

[11]: Antonio L. M. , Antonio T., Juan G. and Jorge E., (2015), Characterization of electron contamination in megavoltage photon beams, Med. Phys. 32 (5), pp 1281-1292.

[12]: IAEA-TECDOC-1603, (2008), The Role of PET/CT in Radiation Treatment Planning for Cancer Patient Treatment, IAEA, VIENNA